

Targeting primary and metastatic tumor growth in an aggressive breast cancer by engineered tryptophan auxotrophic *Salmonella* Typhimurium

Vijayakumar Jawalagatti,^{1,2} Perumalraja Kirthika,^{1,3} and John Hwa Lee¹

¹Department of Veterinary Public Health, College of Veterinary Medicine, Jeonbuk National University, Iksan 54596, South Korea

The global cancer burden is growing and accounted for 10 million deaths in 2020. The resurgence of chemo- and radiation resistance have contributed to the treatment failures in many cancer types. Therefore, alternative strategies are desired for the effective cancer therapy. Bacteria-mediated cancer therapy presents an attractive alternative option for the treatment and diagnosis of cancers. Herein, we describe an engineered *Salmonella* Typhimurium (ST) auxotrophic for tryptophan as a cancer therapeutic. The tryptophan auxotrophy was sufficient to render ST avirulent and highly safe to mice. The auxotroph recovered from the infected tumors had improved ability to target and colonize the tumors. We show that tryptophan auxotrophy reduced the fitness of ST in healthy tissues, but not in the tumors. We evaluated the auxotroph in highly aggressive metastatic 4T1 breast cancer model to inhibit primary tumor growth and lung metastases. The therapy greatly suppressed the primary growth with tumor-free survival of 40% mice. Importantly, therapy abolished the metastatic dissemination of tumor to lungs. Further, therapy markedly diminished the macrophage population in the tumors that may have contributed to the therapeutic benefit recorded. Collectively, results highlight the therapeutic efficacy of the tryptophan auxotrophic ST in an aggressive metastatic cancer model.

INTRODUCTION

Over the years, although the discovery of novel cancer therapies has helped to improve the overall quality of life,¹ many of the therapies are toxic or proven ineffective.²⁻⁴ Further, resurgence of chemo- and radiation-resistant cancers have contributed to the treatment failures in many cancer types.⁵⁻⁷ Moreover, presence of hypoxic and necrotic regions in the tumor limits the response to cancer therapy, leading to treatment failures. A combination of different therapies is mostly employed to treat the cancer to increase the chances of positive outcome. Therefore, alternative strategies are desired for the effective cancer therapy.

The Coley's toxins, although shown to effectively cure cancer several decades ago, did not receive widespread recognition, and with the advent of radiotherapy and chemotherapy, studies were stalled.⁸ However, the research on bacteria-mediated cancer therapy

(BMCT) has gained momentum in the recent past, and several bacterial species have been demonstrated to elicit antitumor effects against a variety of cancers both *in vitro* and *in vivo*.⁹ *Salmonella* Typhimurium (ST), one of the well-studied bacterial strains in cancer therapy, being a facultative anaerobe, can invade and replicate in both well-oxygenated and hypoxic regions of tumors. Further, availability of tools to modify the genome of ST,¹⁰ and for high-throughput screening of mutants,¹¹ provides with opportunities to create strains with excellent safety profile without compromising the tumor-targeting ability.

Although many ST mutants have been evaluated in cancer therapy, VNP20009, A1-R, and Δ ppGpp are the most widely studied strains.¹² The VNP20009 strain was created by chemical and UV mutagenesis and attenuated by purine auxotrophic mutations.¹³ Lipid A was modified to further reduce the virulence of VNP20009. With promising results in preclinical cancer models, strain was evaluated in a phase I clinical trial in 2001.¹⁴ The administration of VNP20009 to patients with metastatic melanoma resulted in poor colonization by the bacteria, and no antitumor effect was noted. In other study, administration of VNP20009 to 4T1 tumor-bearing mice did not result in significant therapeutic benefit on primary tumor size or lung metastases.¹⁵ As strain was created by mutagenesis, several other deletions have also been discovered, including 50 nonsynonymous single-nucleotide polymorphisms (SNPs) and a 108-kb *Suwwan* deletion.¹⁶ However, it is not clear whether these mutations are contributing or hindering the tumor-targeting ability of the VNP20009. Like VNP20009, A1-R was engineered by chemical mutagenesis but was selected for leucine and arginine auxotrophy.¹⁷ A1-R has been successfully used to treat many tumor types in nude-mouse models, including prostate cancer, pancreatic cancer, glioma, breast cancer brain metastasis, and cervical cancer.¹⁸ Of note, A1-R strain has not

Received 7 December 2021; accepted 7 May 2022;
<https://doi.org/10.1016/j.omto.2022.05.004>

²Present address: Department of Biochemistry and Molecular Biology, Mayo Clinic, Rochester, MN 55905, USA

³Present address: Department of Urology, Mayo Clinic, Rochester, MN 55905, USA

Correspondence: John Hwa Lee, Department of Veterinary Public Health, College of Veterinary Medicine, Jeonbuk National University, Iksan 54596, South Korea.

E-mail: johnhlee@jbnu.ac.kr

been evaluated in a 4T1 breast cancer model to inhibit primary tumor or lung metastases. Although proven highly effective, to date, *Salmonella*-based cancer therapeutic has only resulted in fewer clinical trials.^{14,19–21} This highlights the need of further studies to create the strains with efficacy, particularly against highly aggressive tumor models.

In the present study, we created a tryptophan auxotrophic ST by a controlled genetic engineering tool to specifically delete the target genes.¹⁰ We recovered the strain after *in vivo* passages to improve the selective and effective targeting of the tumor. The strain demonstrated excellent safety with no adverse events noted in the infected mice. We evaluated the auxotroph in highly aggressive metastatic 4T1 breast cancer model to inhibit primary tumor growth and lung metastases. The therapy significantly reduced the lung metastases and resulted in tumor-free survival of 40% mice. We observed a drastic reduction in macrophages in the tumor because of *Salmonella* therapy. Collectively, results highlight therapeutic efficacy of the tryptophan auxotrophic ST in aggressive metastatic cancer model. In addition, findings have implications for the development of safe and efficacious bacteria-mediated cancer therapeutics.

RESULTS

Deletion of *trpA* and *trpE* genes render tryptophan auxotrophy to *Salmonella* Typhimurium

To develop an effective and safe bacterial strain for cancer therapy, we created a tryptophan auxotroph ST by deleting genes encoding tryptophan synthase (*trpA*) and anthranilate synthase (*trpE*). The resultant strain was designated as JOL2514. The gene deletions were confirmed by PCR using primers to amplify flanking (outer primer) and DNA-coding regions (inner primer) (Figure S1). The absence of *trpA* and *trpE* mRNA expression was confirmed by an RT-PCR assay (Figure 1C). To validate the auxotrophy, the strain was grown in minimal media with and without the supplemented tryptophan. The strain did not show any visible growth in minimal media; however, upon tryptophan addition, the growth of the auxotroph was restored, thus confirming the tryptophan auxotrophy (Figures 1A and 1B). Further, the deletions did not cause any growth defects, as determined by growth curve analysis of auxotroph in Luria-Bertani (LB) broth (Figure 1D). The results collectively suggested deletion of *trpA* and *trpE* rendered ST auxotrophic for tryptophan and the auxotrophy did not affect the growth in LB broth.

In vivo passage

We initially tested the auxotroph to elicit antitumor effects *in vitro* and *in vivo*; surprisingly, *Salmonella* therapy did not eventuate in anti-cancer effects (data not shown). We thought poor invasion might be the cause for such observation. Therefore, we hypothesized that the repeated passage of the auxotroph *in vivo* may aid in circumventing the problem. Accordingly, we carried out three *in vivo* passages in tumor-bearing mice. The strain was recovered from the tumor after 3 days for the first passage and at 24 h post-inoculation from the subsequent passages to obtain the strain with highest affinity to the tu-

mor. The *trpA* and *trpE* gene deletion in auxotroph was established after each passage by PCR. The passaged strain was designated as ST2514P3 and preserved as glycerol stocks at -80°C . Freshly revived strain was used in each subsequent experiment.

In vivo passage contributed to the enhanced adhesion and invasion

We firstly investigated whether *in vivo* passage altered the bacterial ability to adhere and invade the 4T1 cells. As expected, the *in vivo* passage greatly enhanced the adhesion and invasion of the auxotroph with recovery of higher colonies even after 24 h post-infection (Figures 2A and 2B). The results of colony counting were further corroborated by fluorescence microscopy using mCherry-expressing auxotroph. We observed higher intracellular mCherry-expressing bacteria in cells infected with ST2514P3 when compared with the parental auxotroph (Figure 2B). The findings indicate that the *in vivo* passage had contributed to the increased ability of the auxotroph to target 4T1 cells.

ST2514P3 elicited anti-cancer effects *in vitro*

Next, we evaluated the induction of *in vitro* anti-cancerous effects by the passaged auxotroph. Firstly, the ability of the passaged strain to inhibit the migration of 4T1 cells in a wound-healing assay was assessed. The closure of the gap was evaluated microscopically after staining cells with the DAPI. The control untreated cells migrated faster to close the gap in contrast to the cells infected with ST2514P3 (Figure 3A). We evaluated the effect of therapy on expression of some of the selected genes by qPCR. We recorded an upregulated *p21* gene expression, while genes encoding *p27*, *p53*, and *RCAS1* were downregulated (Figure 3B). Among the cytokine genes studied, tumor necrosis factor alpha (*TNF- α*) expression was highly upregulated when compared with other cytokines (Figure 3C). Lastly, we studied the induction of apoptosis in 4T1 cells infected with ST2514P3. We detected significantly higher number cells in early apoptosis (annexin V⁺) and late apoptosis (annexin V⁺ PI⁺) in 4T1 cells infected with ST2514P3 (Figure 3D). Collectively, *in vitro* results demonstrated the induction of potent anti-cancerous effects by the therapy.

Tryptophan auxotrophy attenuated the *Salmonella* Typhimurium

Safety is one of the major concerns with live-attenuated bacterial therapy. Therefore, we assessed the safety of ST2514P3 in mice following systemic infection via the intraperitoneal route. A group of mice were administered with 1×10^6 colony-forming units (CFUs) weekly for 4 weeks, and the animals were sacrificed 2 weeks after the final dose to determine the bacterial counts in spleen, liver, and lungs. The treatment did not affect the weight gain in mice. No bacterial colonies were recovered from all the organs collected at the end of experiment. On gross examination, no abnormal changes were evident in the spleen of treated mice (Figure 4A). In addition, lung samples were subjected to H and E staining to study the impact of therapy on the histological architecture. Repeated bacterial inoculation did not cause any histopathological changes in the lungs when compared with the untreated controls (Figure 4B). Further, to verify the attenuation, we infected two groups of mice with either the passaged auxotroph or the wild-type *Salmonella* with 5×10^7 CFUs once and

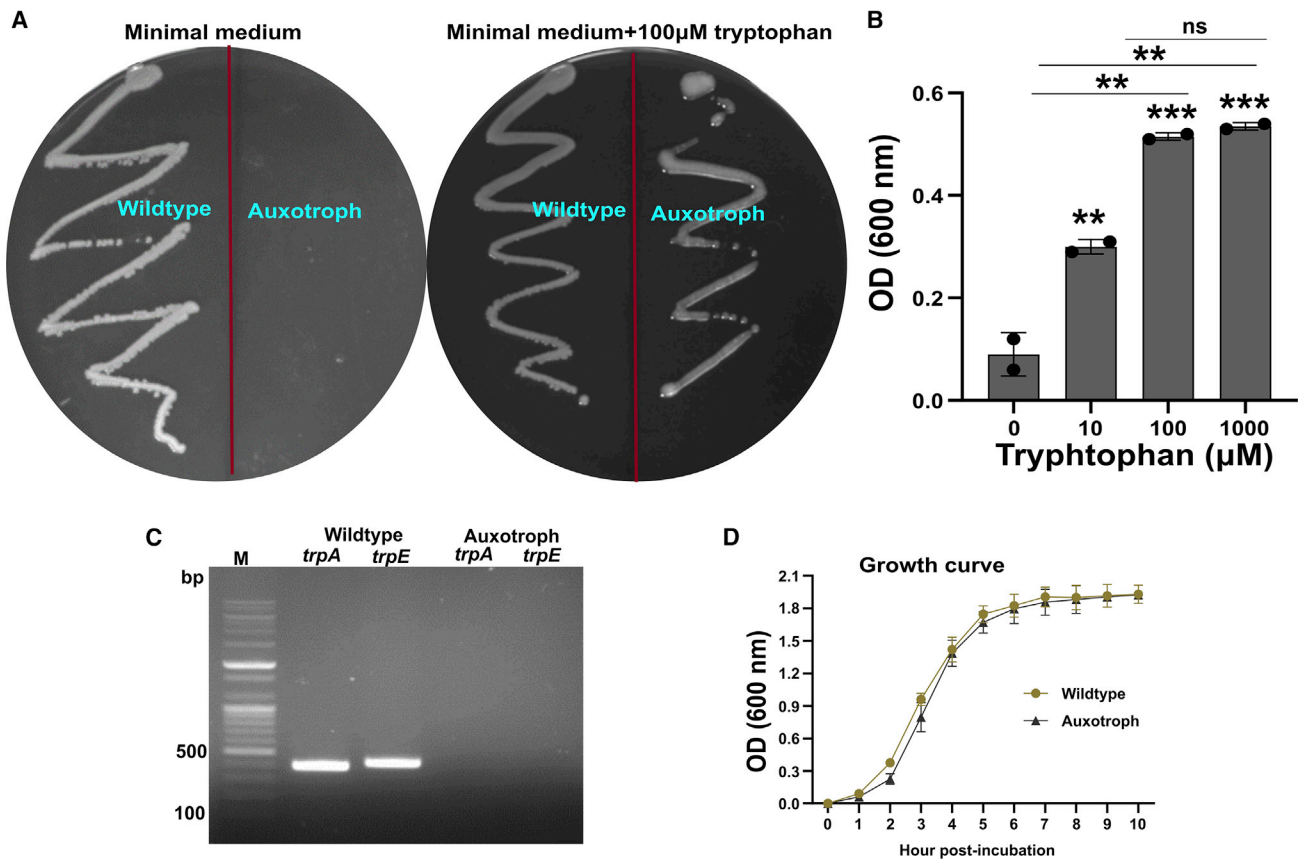


Figure 1. Confirmation of tryptophan auxotrophy following *trpA* and *trpE* gene deletions

Salmonella Typhimurium was rendered tryptophan auxotroph by deleting genes encoding *trpA* and *trpE* by lambda red recombineering. (A) Minimal medium agar plates show growth of wild-type and tryptophan auxotroph strains. The auxotrophy was confirmed by growing the mutant strain in minimal medium and minimal medium supplemented with 100 μM tryptophan. Note the lack of growth of the auxotroph grown only in minimal medium. The tryptophan addition restored the growth of auxotroph. (B) Growth of auxotroph at different tryptophan concentrations is shown. Auxotroph was grown in minimal medium supplemented with different concentrations of tryptophan, and growth was recorded by measuring optical density 600 (OD600). Supplementation of tryptophan at 10 μM was sufficient to revive the growth, and no further increase in growth was evident over 100 μM tryptophan. Data were analyzed by ANOVA using Tukey's post hoc test. ^{ns}p > 0.05; ^{**}p < 0.01; ^{***}p < 0.001. ns, not significant. The data points represent the individual value and error bars denote the SEM (C) Absence of *trpA* and *trpE* gene expression in the auxotroph was determined by RT-PCR using gene-specific inner primers. M, 100 bp plus DNA molecular weight marker. (D) Growth curve of auxotroph grown in LB broth in a shaking incubator at 37°C is shown. The results were compared with the wild-type strain.

observed for mortality. Mice infected with the wild-type *Salmonella* experienced severe disease and died within 10 days (Figure 4C). On the contrary, mice infected with passaged auxotroph did not exhibit any disease symptoms, and no mortality was recorded, indicating the highly attenuated nature of the auxotroph. These results suggested that the tryptophan auxotroph was safe and well tolerated by the mice even after weekly inoculations.

ST2514P3 has reduced fitness in healthy tissues, but not in tumor

The tumor-bearing mice were infected with the ST2514P3 (1×10^6 CFUs, intraperitoneally), and the bacterial colonization in liver, spleen, lung, and tumor samples was evaluated on days 1, 3, 5, 7, and 14 post-infection. The auxotroph was detected in all organs as early as 24 h, and although moderate, the bacterial counts increased

from day 3–5 in liver, spleen, and lung; however, a marked reduction in bacterial number was evident in these organs on day 7, and by day 14, no bacteria were recovered (Figure 5). Contrastingly, bacteria accumulated with increasing number in tumors, and higher bacterial load was recovered for up to day 14. Further, increased tumor-targeting ability of the passaged strain was confirmed by comparing the bacterial recovery from the tumors infected with the parental strain (Figure 5B). These results imply the preference of the auxotroph to selectively colonize the tumor, as tumor microenvironment provides a rich source of tryptophan that is otherwise not seen in healthy tissues.

ST2514P3 targeted both primary tumor growth and lung metastases

The 4T1 serves as a model for type IV breast cancer and has been extensively used in preclinical studies.^{22–24} The 4T1 cells produce

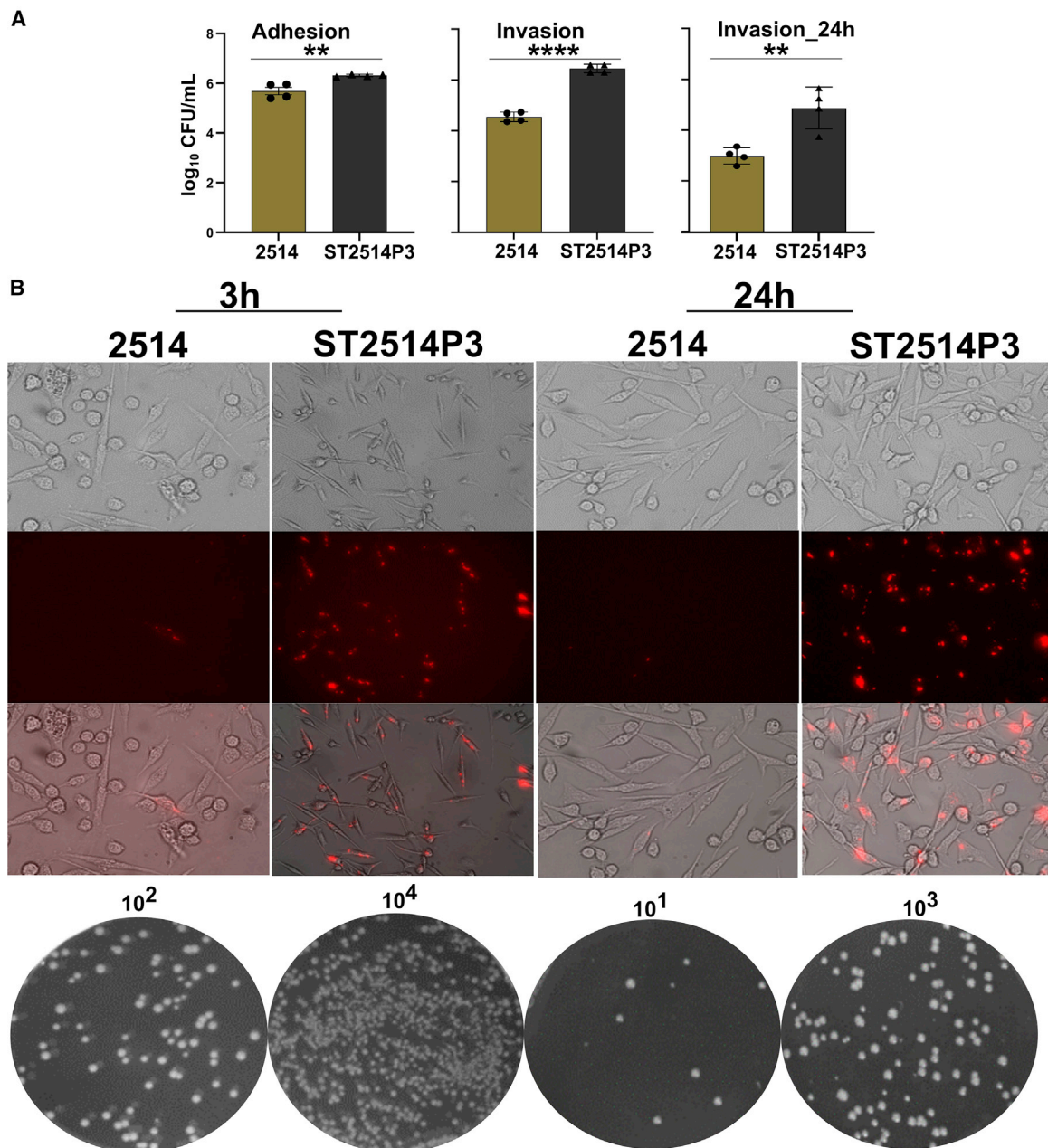


Figure 2. Evaluation of influence of *in vivo* passage on 4T1 cell adhesion and invasion by the ST2514P3

The tryptophan auxotroph was passaged *in vivo* in tumor-bearing mice thrice. The *in vivo* passaged strain, ST2514P3, was evaluated in adhesion and invasion assays using 4T1 cells, and the results were compared with the parental auxotroph, JOL2514. 4T1 cells were seeded in the 24-well plates at 1×10^5 cells per well and allowed to grow for 24 h. *Salmonella* strains growing at mid-log phase were harvested by centrifugation (3,500 rpm, 15 min) and washed once with PBS. The bacterial number was enumerated by OD600, and 4T1 cells were infected at 10 MOI. (A) Adherent bacteria quantified after 30 min of infection are shown. Invading bacteria were quantified at 3 and 24 h post-infection. For invasion assay, external bacteria were killed by addition of gentamicin after allowing the bacteria to invade the cells. Bacterial counts were enumerated by plating decimal dilutions on LB agar plates. Data were analyzed by t test. ** $p < 0.01$; **** $p < 0.0001$. The data points represent the individual value and error bars denote the SEM. (B) Intracellular mCherry-expressing bacteria as visualized by a fluorescence microscope are shown. Note the rod-shaped bacteria within the cytoplasm of infected 4T1 cells. Representative agar plates are shown at the bottom.

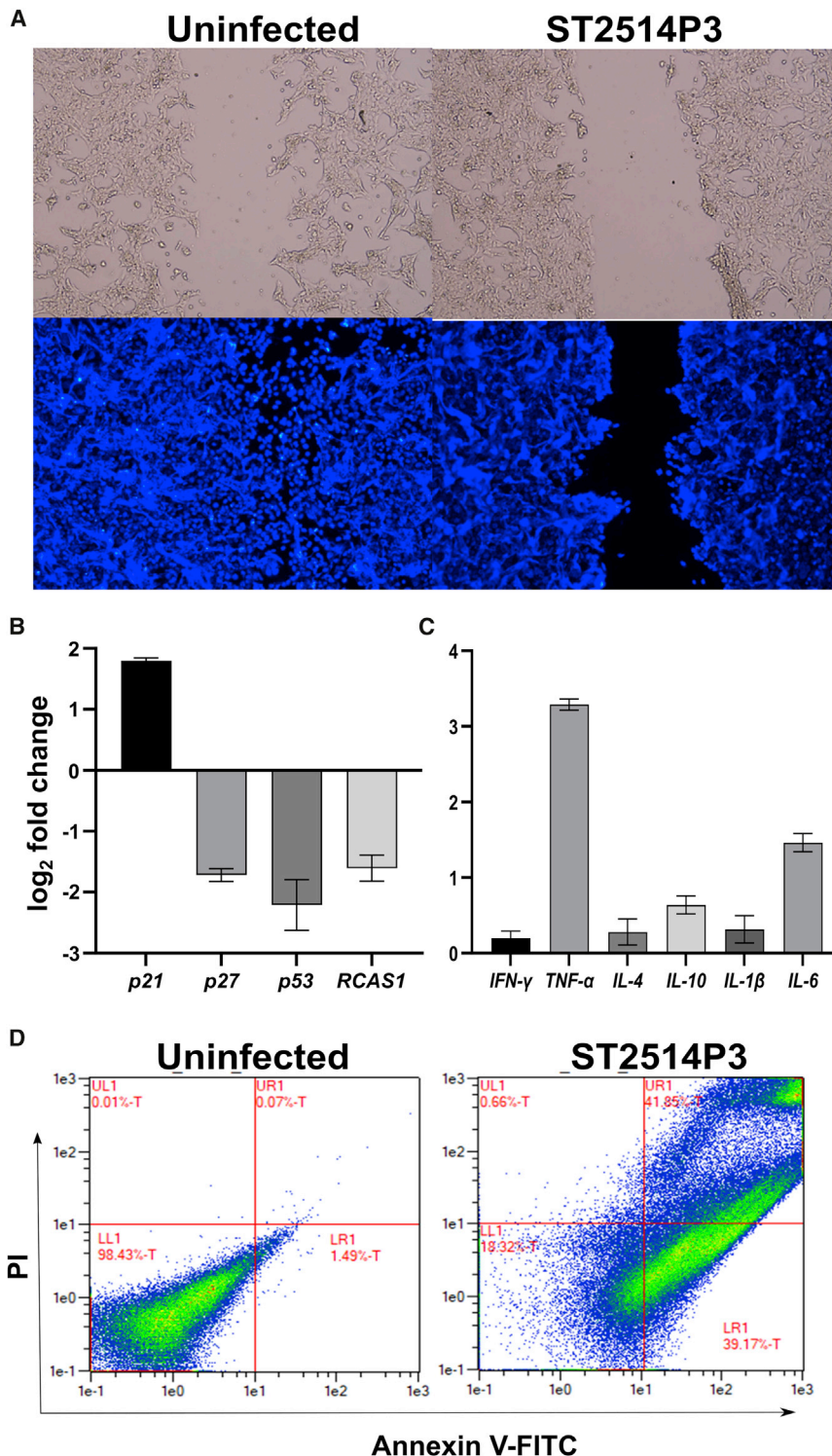


Figure 3. Analysis of anti-cancerous effects of ST2514P3 *in vitro*

(A) Inhibition of 4T1 cell migration in a wound healing assay. 4T1 cells were grown in ibidi cell culture inserts for wound healing assay and infected with the passaged tryptophan auxotroph, ST2514P3. After allowing the bacteria to invade 4T1 cells, external bacteria were killed by gentamicin treatment. Closure of the wound was observed microscopically after 48 h by DAPI staining of the nucleus. Uninfected cells served as controls. The bright-field image denotes the pre-infection time point. (B) The expression of *p21*, *p27*, *p53*, and *RCAS1* in infected cells by qPCR is shown. (C) Expression of cytokine genes by qPCR is shown. For qPCR assay, cells were collected 24 h post-infection and RNA was extracted. Error bars denote the SEM. (D) Fluorescence-activated cell sorting (FACS) plots show apoptotic 4T1 cells. 4T1 cells infected as earlier were collected after 24 h. The adherent and non-adherent cells were stained using propidium iodide (PI) and annexin V-FITC and analyzed on a FACS reader. Uninfected cells served as controls.

BALB/c mice aged 6–8 weeks were inoculated with 1×10^5 4T1 cells into the 2nd mammary fat pad using a wide bored needle. Palpable tumors developed within a week, and at day 10, tumor volume was recorded and animals were divided into two groups of 10 mice each. One group of mice was treated with 1×10^6 CFUs ST2514P3 via the intraperitoneal route. Mice were administered a total of four doses at weekly intervals (Figure 6A). The other group of mice served as untreated placebo control. The treatment suppressed the growth of primary tumor, with complete disappearance observed in four mice (Figures 6B–6D), although, in the placebo group, tumors grew continuously during the study. Consistent with the primary tumor growth, spleen from placebo controls weighed more than the spleens from treated mice (Figure 6E).

Next, we studied the histological changes in the primary tumors after hematoxylin and eosin (H&E) staining. On histological examination, the tumors from treated mice had diffused areas of necrosis characterized by lost cellular integrity (Figure 6F). To further verify the impact of *Salmonella* therapy on the tumor histology, we analyzed the samples collected on different days after infection

tumors consistently in immunocompetent BALB/c mice and spontaneously metastasize to lung and other organs.²⁵ Therefore, we evaluated the therapeutic benefits of the therapy in this model. Female

during biodistribution experiment by H&E staining. We observed a consistent large whitish area of necrosis in the treated tumors as early as day 1, and the necrosis appeared to be maximum on day

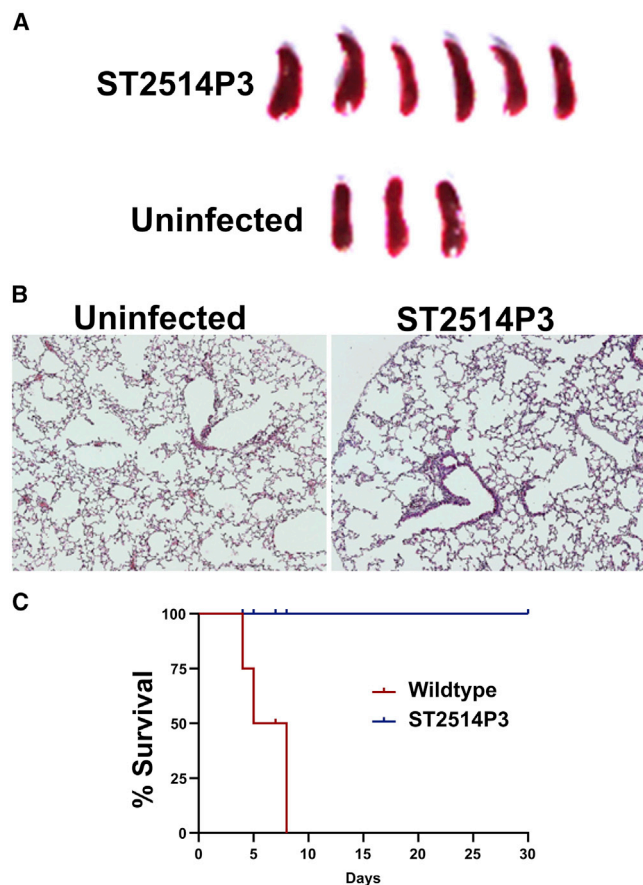


Figure 4. Evaluation of safety of ST2514P3 in mice

(A) Gross appearance of spleen. Mice ($n = 6$) were infected with the passaged auxotroph, ST2514P3 intraperitoneally at 1×10^6 CFUs. Mice were administered four doses every week. Mice ($n = 3$) served as uninfected controls. Mice were sacrificed 2 weeks after the final dose, and spleen samples were examined for gross changes, such as enlargement. (B) H&E-stained lung sections are shown. Lungs collected at the end of experiment were analyzed by H&E staining to study histological changes. Therapy did not affect the histological architecture of lungs. (C) Survival graph is shown. Two groups of mice were infected with either ST2514P3 or the wild-type strain with 5×10^7 CFUs and were observed for survival and mortality.

14 (Figure S2). On the contrary, the untreated tumors had higher areas of viable tumor cells.

An estimated 90% deaths in breast cancer are due to metastatic dissemination of tumor, with lung being the most commonly involved organ.²⁶ Therefore, we determined the effect of therapy on lung metastases by gross, histological, and negative staining methods. On gross and histological examination, lungs of treated animals did not show any evidence of metastases, whereas several metastatic foci were detected in the placebo controls (Figure 6G). The metastatic infiltrating tumor nodule and cells were detected in the H&E-stained lungs of placebo controls. Further, numerous metastatic nodules were observed in the lungs of placebo controls stained with 10% nigrosine dye, while no nodules were evident in the lungs of treated mice (Fig-

ure 6H). Altogether, findings highlighted the potent anti-cancerous effect of tryptophan auxotroph ST therapy culminating in the inhibition of primary and metastatic tumor growth.

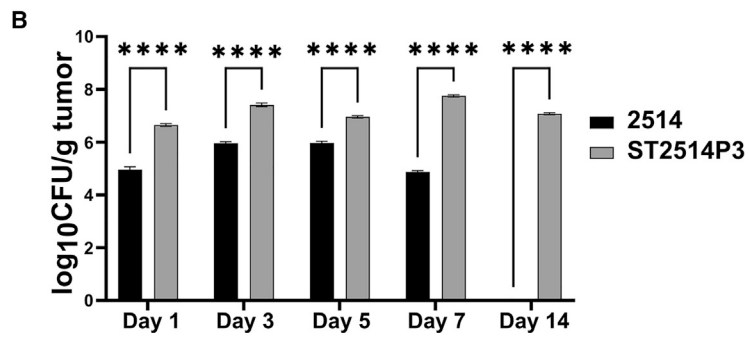
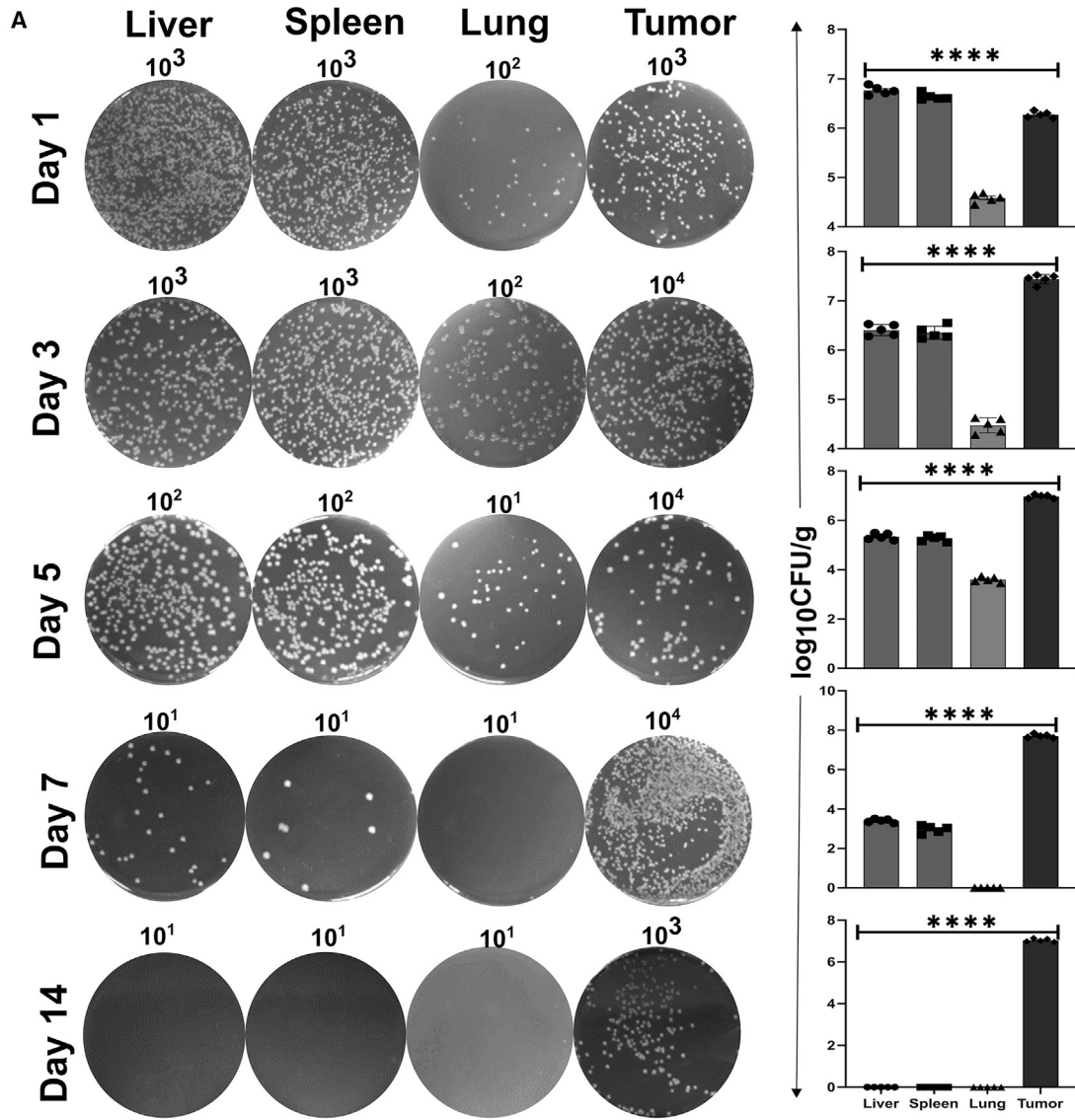
Therapy caused a drastic reduction in macrophage cell markers

The tumor microenvironment plays a crucial role in aggressive behavior of tumors;²⁷ therefore, to understand the effect of therapy on macrophage population in the tumor, immunohistochemistry (IHC) was carried out. We studied the expression of selected macrophage markers, such as CD68, CD206, iNOS, and CCL2. We detected increased expression of all the markers in tumors from untreated placebo mice (Figure 7). Contrarily, the *Salmonella* therapy significantly blunted the expression of all the markers in the tumor. The findings suggest the limitation of macrophage infiltration into the tumor in response to *Salmonella* therapy.

DISCUSSION

Bacteria-mediated cancer therapy (BMCT) presents an effective alternative option for the treatment and diagnosis of cancers.^{28,29} Herein, we describe an engineered *Salmonella* Typhimurium (ST) to selectively target and kill mammary cancer cells. Moreover, no reports exist on the evaluation of tryptophan auxotroph as a therapy against any kind of cancer. The approach is based on the inactivation of *trpA* and *trpE* genes in the tryptophan biosynthesis pathway to create auxotrophic *Salmonella* that has reduced fitness in the healthy tissues. We carried out three sequential *in vivo* passages in tumor-bearing mice to further improve the preferential colonization of tumors by the *Salmonella*. As expected, the *in vivo* passage enhanced the ability of the auxotroph to invade and proliferate in 4T1 cells. Further, the auxotroph accumulated in increased numbers in the tumors, owing to the *in vivo* passage. This may be attributed to the establishment of induced memory response to the tumor by the repeated passage.³⁰ Previously, studies have documented the influence of nutrient availability and environmental stress factors in bacterial memory mechanisms.^{30–32} Importantly, the memory establishment was not linked to genotypic alterations and was stable for over several generations in absence of the memory stimulus.³⁰

We created a tryptophan auxotrophic ST with an aim to attenuate the *Salmonella* and to reduce its fitness in healthy tissues. Likewise, the tryptophan auxotrophy dramatically reduced the ability of the ST to survive and propagate in the healthy tissues, and the bacteria were cleared by day 7–14, even in the absence of an antibiotic therapy. Further, the auxotroph caused minimal or no impact on liver, spleen, and lungs. Moreover, the magnitude of attenuation caused by tryptophan auxotrophy was at least 5,000-fold. However, the auxotroph continued to grow in tumors for up to 14 days with recovery of higher bacterial counts on day 7. This discrepancy in colonization could be explained by limited or unavailability of free tryptophan in healthy tissues, due to which auxotroph cannot survive for longer duration in these tissues. However, tumors serve as nutrient rich sinks,^{33,34} enabling the proliferation of auxotroph. In agreement, a leucine-arginine auxotroph was shown to selectively colonize prostate cancer cells with recovery of a larger number of bacteria from tumors than the



(legend on next page)

healthy organs.^{17,35} The reduced fitness of the strain in healthy tissues may further be attributed to excellent safety observed for mice. Our findings suggest that the tryptophan auxotrophy was sufficient to render ST avirulent to mice and contributed to increased colonization of the tumor.

Although major developments in cancer diagnosis and therapy have contributed to the improved outcomes in cancers, the global cancer burden was predicted to increase.³⁶ Due to the fact that acquired resistance to radiation and chemotherapeutics is rampant and most cancer therapies pose toxicity threat, alternative strategies would bolster the existing cancer therapies. Therefore, we studied the ability of the engineered tryptophan auxotroph to induce anti-cancerous effects in a highly aggressive breast cancer model. Further, 4T1 model spontaneously metastasizes to lungs and provides a more natural way of studying metastases. The primary tumor growth was greatly suppressed in the treated mice with tumor-free survival of 40% mice, suggesting the ability of the auxotroph to target and kill cancer cells. Most importantly, therapy prevented the metastatic dissemination of tumor to lungs, even in the mice with visible primary tumor growth. In a previous study using VNP20009 ST, authors did not observe the therapeutic benefit in preventing the lung metastases.¹⁵ On the contrary, tumor-bearing mice infected with VNP20009 evidenced exacerbated disease and died earlier than the controls. Therefore, the findings have important implications for the development of BMCT in treating and preventing the metastatic spread of cancer cells.

The development of VNP20009 and A1-R, two of the well-studied strains, relied on mutagenesis to create the tumor-targeting avirulent ST strains, whereas we created the tryptophan auxotroph by a controlled gene-deletion tool.¹⁰ Because of the non-targeted nature of mutagenesis, the strains likely to harbor other mutations, such as presence of 50 nonsynonymous SNPs and a 108-kb *Suwwan* deletion in VNP20009.¹⁷ Whether these mutations contribute or hinder the tumor targeting is not clear. Further, it is not known whether these mutations influenced the outcome that no anti-cancerous effect was observed in malignant melanoma patients treated with VNP20009 in a phase I clinical trial. Therefore, development of strains with known genotype and having specific gene deletions are highly desired.^{15,37} Moreover, creation of auxotrophic mutants by gene deletion would be stable and have lesser or no chance of reverting back to wild type.

The components of tumor microenvironment play a crucial role in aggressive behavior of tumors; in particular, the role of macrophages, cancer-associated fibroblasts, and endothelial cells in promoting tu-

mor progression has been well established.²⁷ We focused on how the *Salmonella* therapy affected the macrophage population within the tumor to gain some insight. We recorded a marked reduction or no expression of CD68, iNOS, CD206, and CCL2, selected markers of macrophages, in the tumors from treated mice. The tumor-associated macrophages (TAMs) generally have pro-tumoral role both in the primary tumor and at metastatic sites.³⁸ TAMs influence the tumor progression by promoting tumor cell motility, invasion, and angiogenesis and by suppressing T cell responses.³⁸ Thus, suppression of TAMs by *Salmonella* therapy might have contributed to the abolition of lung metastases in these mice. The fact that we detected high macrophage population in the tumors of placebo controls was not surprising, as macrophages can make up as much as 50% cell mass in breast cancer.^{39,40} Further, macrophage density has been associated with the poor prognosis in many cancer types.^{41–44} It would be interesting to dissect the mechanism by which *Salmonella* therapy has contributed to the limitation of TAMs and whether necrosis had any role. Although finding seems to provide an alternative strategy to target TAMs, more studies and in different cancer types are required to understand the mechanism before *Salmonella* could be developed as a therapy targeting TAMs.

In summary, we have created a tryptophan auxotrophic ST as a cancer therapeutic. The *in vivo* passage contributed to the improved ability of the auxotroph to target cancer cells. The auxotroph colonized the tumors in increasing numbers than the healthy tissues. The tryptophan auxotroph demonstrated potent anti-cancerous effects as a monotherapy with cancer-free survival of 40% mice in a highly aggressive breast cancer model. Further, therapy markedly reduced the macrophage population in the tumors. Collectively, results document the attenuation of ST by tryptophan auxotrophy and that the therapy culminated in significant cancer therapeutic benefits. In addition, findings provide novel insights into engineering bacteria in cancer therapy.

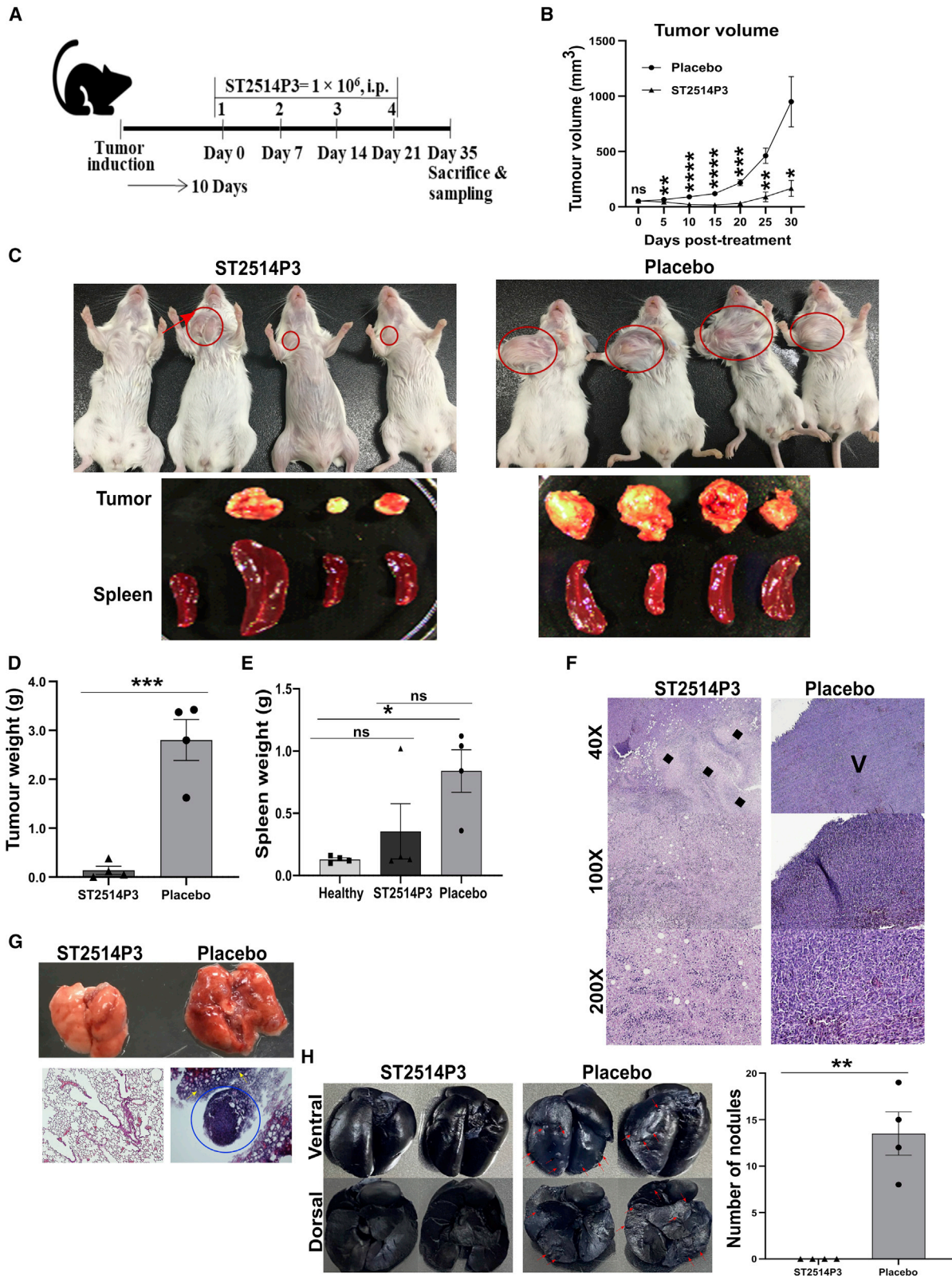
MATERIALS AND METHODS

Ethics statement

Female BALB/c mice, aged 6 weeks and specific pathogen free (SPF), were obtained from Koatech in Pyeongtaek, Korea. Mice were maintained on a standard feeding regimen with a 12-h light-dark cycle at the Animal Housing Facility of the College of Veterinary Medicine, Jeonbuk National University. Animal experiments were approved by the Jeonbuk National University Animal Ethics Committee (JBNU 2021-027) under Korean Council on animal care and the Korean Animal Protection Law, 2001, article 13.

Figure 5. Analysis of localization of ST2514P3 in different organs of mice

(A) Tumor-bearing mice were infected with the passaged auxotroph, ST2514P3, intraperitoneally at 1×10^6 CFUs. At days 1, 3, 5, 7, and 14 post-infection, five mice were sacrificed to study the colonization of ST2514P3 in lung, liver, spleen, and tumor. The samples were weighed and homogenized in PBS. Decimal dilutions of the homogenates were plated on LB agar. A representative agar plate at specified dilution has been shown. The quantitative bacterial counts were determined, and the data in \log_{10} CFU/g have been presented in the right panel. The data represent five mice per time point. (B) Bar diagram depicting the improved tumor-targeting ability of the passaged auxotroph over the parental auxotroph is shown. Data were analyzed by ANOVA. ****p < 0.0001. The data points represent the individual value from each mouse and error bars denote the SEM. CFU, colony-forming units.



(legend on next page)

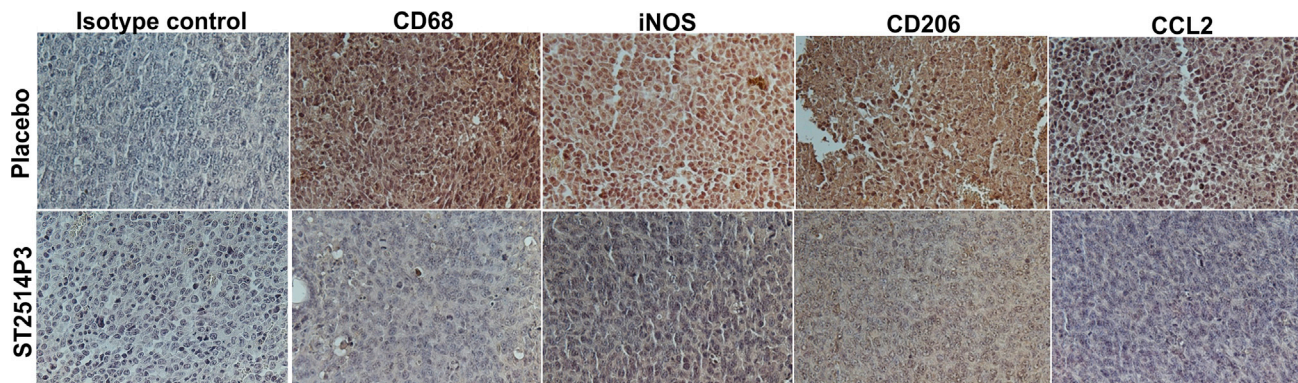


Figure 7. Immunohistochemical analysis of macrophage markers

Shown here are the representative images of tumor samples stained with selected macrophage markers, such as CD68, iNOS, CD206, and CCL2. Higher number of positive cells were detected in tumors of placebo controls. Note the marked reduction in positive cells in tumors from mice treated with passaged tryptophan auxotroph, ST2514P3.

Cell line

4T1 mouse mammary carcinoma cell line was a kind gift from Dr. Hunjoo Ha, Graduate School of Pharmaceutical Sciences, Ewha Womans University, Seoul. The cell line was maintained in RPMI (Lonza, Switzerland) supplemented with 10% fetal bovine serum (Gibco, USA), 100 U/mL penicillin, and 100 μ g/mL streptomycin at 37°C in 5% CO₂.

Bacterial strains, plasmids, and primers

Table 1 summarizes the strains of bacteria, plasmids, and primers used in this study. The bacteria were grown in LB broth (Becton Dickinson, USA) with agitation at 37°C using appropriate antibiotics whenever applicable. For bacterial enumerations, Brilliant Green Agar plates (Becton Dickinson, USA) were used.

Construction and characterization of tryptophan auxotrophic *Salmonella Typhimurium*

Genes encoding tryptophan synthase (*trpA*) and anthranilate synthase (*trpE*) were deleted from ST genome by lambda red recombination.¹⁰ Briefly, wild-type ST (JOL 401) was transformed with a helper plasmid, pKD46, which provides lambda red components required for homologous recombination. The target gene *trpA* was replaced with the *cat*^R gene contained on a linear PCR product ampli-

fied from the pKD3 plasmid. Recombinant clones were selected by plating on LB broth containing 35 μ g/mL chloramphenicol. The knockout was confirmed by PCR using flanking (outer) and gene-specific (inner) primer sets listed in Table 1. The antibiotic resistance cassette was eliminated using the helper plasmid, pCP20. Following removal of the antibiotic cassette, *trpE* gene was knocked out in similar fashion. The mutant was subjected to *in vitro* growth curve analysis and tryptophan auxotrophy. The mutant was grown in 20 mL LB broth, and the growth was followed for up to 12 h. To validate the tryptophan auxotrophy, mutant was grown in M9 minimal medium⁴⁷ with and without supplemented tryptophan (Sigma, USA) and incubated overnight at 37°C.

Adhesion and invasion assays

Adhesion and invasion assays were carried out as described previously.⁴⁵ Briefly, 4T1 cells were grown to 85% confluence and infected with mutant at MOI of 1:10. After 30 min, adherent bacteria were enumerated by spreading infected cells on LB plate. For invasion assays, 2 h post-infection, the cell monolayers were treated with culture medium containing gentamicin (150 μ g/mL) to eliminate any extracellular bacteria. Then, the cells were lysed with 0.25% trypsin-EDTA and 0.1% Triton X-100 and spread on LB agar plates using decimal dilutions. Also, invasion was determined by

Figure 6. Assessment of therapeutic potential of the therapy in an aggressive 4T1 breast cancer model

(A) Schematic presentation of therapy schedule. 4T1 cells growing in T75 flasks were harvested and quantified by trypan blue dye exclusion. Mice were induced for tumor formation by inoculating 1×10^5 4T1 cells into the second mammary fat pad. The tumor size was recorded at day 10 post-tumor induction, and one group of mice ($n = 10$) were administered with four ST2514P3 therapies at weekly intervals. Second group ($n = 10$) of mice served as placebo controls and received same volume of sterile PBS. Tumor size was measured regularly using Vernier caliper. Mice were sacrificed 2 weeks after the final treatment to study the therapeutic benefit. (B) Tumor volume recorded over the course of the study is shown. Data were analyzed by two-way ANOVA using Šídák's post hoc test for multiple comparisons. ^{ns} $p > 0.05$; ^{**} $p < 0.01$; ^{***} $p < 0.001$; and ^{****} $p < 0.0001$. Error bars denote the SEM. (C) Representative photographs show tumors in mice and gross appearance of isolated tumors and spleens. Note the reduction of tumor size following therapy. (D and E) Tumor (D) and spleen (E) weight in grams (g) are plotted. Tumor weight data were analyzed by t test and spleen weight data by ANOVA using Tukey's post hoc test. ^{ns} $p > 0.05$; ^{*} $p < 0.05$; and ^{***} $p < 0.001$. (F) Representative H&E-stained pictures of tumor sections are shown. Note the extensive necrosis in treated mice (black rhombus). V, viable tumor region. (G) Gross and histological appearance of lung metastases is shown. Note the metastatic tumor nodule (blue circle) and infiltrating tumor cells (yellow arrow) in lung of placebo control mice. (H) Nigrosine dye-stained ventral and dorsal view of lungs show metastatic nodules. Note the numerous nodules (red arrows) in the lungs of placebo mice. Nodule numbers counted are plotted in the right panel. Data were analyzed by t test. ^{**} $p < 0.01$. In (D), (E) and (H), the data points represent the individual value from each mouse and error bars denote the SEM.

Table 1. List of bacterial strains, plasmids, and primers used in the present investigation

Bacteria/plasmid	Genotypic characteristics	Reference
<i>S. Typhimurium</i>		
JOL401	<i>Salmonella</i> Typhimurium wild type, SPI-1 <i>invAE⁺hilA⁺avr⁺</i> ; SPI-2, amino acid permease; SPI-3, <i>mgtC⁺</i> ; SPI4, ABC transporter; SPI5, <i>pipB⁺</i>	lab stock
JOL2514	JOL401Δ <i>trpA</i> Δ <i>trpE</i>	this study
ST2514P3	thrice <i>in vivo</i> passaged JOL2514	this study
Plasmids		
pKD46	oriR101-repA101ts; encodes lambda red genes (exo, bet, gam); native terminator (tL3); arabinose-inducible promoter for expression (ParaB); bla	Datsenko and Wanner ¹⁰
pKD3	oriR6Kgamma, bla (ampR), rgnB (Ter), catR, FRT	Datsenko and Wanner ¹⁰
pCP20	encodes FLP, ampicillin ^R and Cm ^R	Datsenko and Wanner ¹⁰
Gene deletion primers		
<i>trpA</i> -pKD3	forward- 5'-TGGCCGCGGAGATAAAGACATCTTTACCGTACACGA TATCCTGAAAAGCGCGTGTAGGCTGGAGCTGCTTC-3' reverse- 5'-ACTCATTAAGCCGCCAGCGTTATGCTGACGGCTTAA CCCGATGGGAATTAGCCATGGTCC-3'	this study (GenBank: NC_003,197.2 and STM1727)
<i>trpE</i> -pKD3	forward- 5'-AACGATACCCGGCCCGCTGTTAAGCGGGCTTTTTTTG AACAAAATAATGTGTAGGCTGGAGCTGCTTC-3' reverse- 5'-CAGGTTCCAGGTAAACGAGTCGATGTTATCGAGCAGCA GAATATCAGCCAATGGGAATTAGCCATGGTCC-3'	this study (GenBank: NC_003197.2 and STM1723)
<i>trpA</i> outer primer	forward- 5'-AGCAACTGCTGGTGGTCAAT-3' reverse- 5'-TTTGAAAAGCTGGACGGGA-3'	this study
<i>trpA</i> inner primer	forward- 5'-TCGTGAAAAACACCCGACCA-3' reverse- 5'-CTGTTCCGGCAGGAGATAC-3'	this study
<i>trpE</i> outer primer	forward- 5'-ATAGCGGGCGGTGTATGAAC-3' reverse- 5'-AGGCGATCGATAAGCGTCTG-3'	this study
<i>trpE</i> inner primer	forward- 5'-ATTGCCGCTACTGGATACCG-3' reverse- 5'-ACTGTTGGCTAAGGTACGCC-3'	this study
qRT-PCR primers		
<i>IFN-γ</i>	forward- 5'-AGACAATGAACGCTACACAC-3' reverse- 5'-TCTTTCTTCCACATCTATGCC-3'	Kirthika et al. ⁴⁵
<i>TNF-α</i>	forward- 5'-CATCTTCTCAAAATTCGAGTGACAA-3' reverse- 5'-TGGGAGTAGACAAGGTACAACCC-3'	Giulietti et al. ⁴⁶
<i>IL-4</i>	forward- 5'-ACGGATGCGACAAAATCAC-3' reverse- 5'-ACCTTGGAAGCCCTACAGAC-3'	Kirthika et al. ⁴⁵
<i>IL-10</i>	forward- 5'-GACAACATACTGTAACCCGAC-3' reverse- 5'-ATCACTCTTCACTGCTCC-3'	Kirthika et al. ⁴⁵
<i>IL-1β</i>	forward- 5'-CAACCAACAAGTGATATTCTCCATG-3' reverse- 5'-GATCCACACTCAGCTGCA-3'	Giulietti et al. ⁴⁶
<i>IL-6</i>	forward- 5'-GAGGATACCACTCCCAACAGACC-3' reverse- 5'-AAGTGCATCATCGTTGTCATACA-3'	Giulietti et al. ⁴⁶
<i>p21</i>	forward- 5'-CGAGAACGGTGGAACCTTTGAC-3' reverse- 5'-CAGGGCTCAGGTAGACCTTG-3'	This study (GenBank: NC_000077.7)
<i>p27</i>	forward- 5'-TCAAACGTGAGAGTGTCTAACGG-3' reverse- 5'-AGGGGCTTATGATTCTGAAAGTCG-3'	This study (GenBank: NC_000077.7)
<i>p53</i>	forward- 5'-GTCACAGCACATGACGGAGG-3' reverse- 5'-TCTTCCAGATGCTCGGGATAC-3'	This study (GenBank: NC_000077.7)
<i>RCAS1</i>	forward- 5'-GGAACAACCTGGAACCTGACTAC-3' reverse- 5'-AAAAACCCGTGCTACCATCTG-3'	this study (GenBank: NM_001357691.1)
<i>GAPDH</i>	forward- 5'-TCACCACCATGGAGAAGGC-3' reverse- 5'-GCTAAGCAGTTGGTGGTGCA-3'	Giulietti et al. ⁴⁶

fluorescence microscopy using mCherry (red)-expressing bacterial strains. For this purpose, strains were transformed with mCherry-expressing plasmid by electroporation at 1.8 kV current, 25 μ F capacitance, and 200 Ω resistance (Harvard apparatus, USA). The positive transformants were selected on ampicillin plates and confirmed by fluorescence microscopy.

In vivo passaging

4T1 tumor cells (1×10^5) were injected subcutaneously into second mammary fat pad of mice and grown for 15 days. Tumor-bearing mice ($n = 2$) were infected with the tryptophan auxotroph at 1×10^6 CFUs via the intraperitoneal route. The mice were sacrificed at day 3 to harvest the bacteria from the tumor by plating on Brilliant Green Agar (BGA). The strain was confirmed by PCR and used in subsequent passage. The mutant was passaged thrice.

Wound healing assay

Wound healing assay was carried out to determine the ability of the mutants to inhibit migration of tumor cells *in vitro*. The assay was performed using ibidi Culture-Inserts (ibidi, Germany). Cells were seeded and allowed to grow for 24 h to form an optically confluent monolayer. The cells were then infected with the bacterial strains at MOI of 10 for 3 h, and extracellular bacteria were killed by gentamicin. The inserts were removed to create the gap, the cells were incubated for 48 h, and results were documented. Cell nucleus was stained by DAPI, and gap filling was observed by a fluorescence microscope.

qPCR

The mRNA levels of selected genes encoding cytokines and cell cycle regulators in 4T1 cells were analyzed post-infection with the bacterial strains. Briefly, the infected cells were harvested 24 h post-infection (hpi). The total RNA was isolated (RiboEx kit, GeneAll Biotechnology, South Korea) and reverse transcribed using strand cDNA Synthesis Kit (Elpis Biotech, South Korea). Transcriptional levels were normalized against *GAPDH* by $2^{-\Delta\Delta CT}$ method.⁴⁸ The experiment was performed using the primers listed in Table 1.

Analysis of apoptosis by flow cytometry

The 4T1 cells were cultured in 10% RPMI in a 24-well plate at 1×10^5 cells/well. The cells were infected with tryptophan auxotroph at 10 MOI for 24 h to study apoptosis using fluorescein isothiocyanate (FITC) Annexin V Apoptosis Detection Kit I (BD Pharmingen, USA), following manufacturer's instructions.

Safety assessment of the mutant

A group of mice ($n = 6$) were administered weekly doses with 1×10^6 CFUs intraperitoneally for 4 weeks. A group of mice ($n = 3$) served as uninfected controls. The animals were sacrificed 2 weeks after the last dose, and tissue samples were collected for gross and histological analysis. Further, bacterial counts were enumerated by plating on BGA. To further verify the safety, two groups of mice were administered with either the passaged auxotroph or wild-type bacteria with 5×10^7 CFUs intraperitoneally once and monitored for the appear-

ance of any disease symptom, weight loss, and mortality for up to 30 days.

Determination of biodistribution of the mutant

4T1 tumor cells (1×10^5) were injected subcutaneously on mammary fat pad of mice and grown for 15 days. The tryptophan auxotroph was grown to logarithmic phase in LB broth, washed and diluted with PBS, and injected intraperitoneally at 1×10^6 CFUs per mouse. The tissue samples ($n = 5$ mice) were obtained from lung, liver, spleen, and tumor at indicated time points post-infection. The tissues were homogenized and supernatants plated on BGA for bacterial recovery. In addition, tissues were fixed in 10% neutral buffered formalin for histological processing.

4T1 mouse tumor model and *Salmonella* therapy

4T1 tumor cells (1×10^5) were injected subcutaneously on mammary fat pad of mice and grown for 10 days. The tumor size was recorded, and mice were randomly divided into two groups of 10 each. One group of mice was administered with four weekly treatments consisting of 1×10^6 CFUs ST2514P3 via the intraperitoneal route in a volume of 100 μ L. The other group of mice served as untreated placebo controls that received 100 μ L sterile PBS. Following treatment, the mice were observed daily and size of tumor measured regularly using Vernier caliper. Tumor volume was calculated using the following formula: tumor volume = (length \times width²)/2. Mice were sacrificed at day 45 (day 35 post-treatment) of the experiment to harvest the tumor, lung, and splenic tissues. The size and weight of the isolated organs were recorded. Lung samples were subjected to gross and histopathological examination to study metastases. Alternatively, lung metastases were determined by nigrosine dye (Sigma, USA) inflation method.

Histopathological analysis

Isolated tumor samples were fixed in formalin for 2 days and subjected to standard tissue processing with paraffin embedding. The sections were stained by H&E.

IHC

Formalin-fixed paraffin-embedded (FFPE) tumor sections were deparaffinized by immersing in two changes of xylene, followed by one immersion in xylene-alcohol (1:1 ratio) for 3 min each.⁴⁹ The sections were rehydrated by immersing in a series of alcohol gradients of 100%, 95%, 75%, and 50% for 3 min each. The sections were washed in tap water and incubated in 3% H₂O₂ in methanol for 10 min to block endogenous peroxidase activity. Following two PBS washes, antigen retrieval was performed by incubating at 100°C for 30 min in 0.5 mM citrate buffer (pH 6.0). Blocking was performed using 3% BSA at room temperature (RT) for 2 h. The sections were incubated with CD68 (cat no. PA5-78996), iNOS (cat no. PA3-030A), CD206 (cat no. PA5-101657), or CCL2 (cat no. MA5-17040) antibodies from Thermo Scientific at 1:200 dilutions overnight at 4°C. Following two PBS washes, goat anti-rabbit immunoglobulin G (IgG) horseradish peroxidase (HRP) or goat anti-mouse IgG was added at 1:3,000 dilutions

and incubated at RT for 1 h. The sections were developed using DAB substrate.

Statistical analysis

The data were analyzed statistically using IBM SPSS and GraphPad Prism v.9. Number of animals used and the statistical tool applied have been described in the respective figure legends. A $p < 0.05$ between the groups was considered significant.

SUPPLEMENTAL INFORMATION

Supplemental information can be found online at <https://doi.org/10.1016/j.omto.2022.05.004>.

ACKNOWLEDGMENTS

This research was supported by Basic Science Research Program through the National Research Foundation of Korea (NRF) funded by the Ministry of Education (2019R1A6A1A03033084).

AUTHOR CONTRIBUTIONS

Conceptualization, V.J. and P.K.; formal analysis, V.J. and P.K.; investigation, V.J. and P.K.; methodology, V.J. and P.K.; writing – original draft, V.J. and P.K.; writing – review & editing, V.J., P.K., and J.H.L.; funding acquisition, J.H.L.; resources, J.H.L. All authors approved the final version of the manuscript.

DECLARATION OF INTERESTS

The authors declare no competing interests.

REFERENCES

- Markham, M.J., Wachter, K., Agarwal, N., Bertagnoli, M.M., Chang, S.M., Dale, W., Diefenbach, C.S.M., Rodriguez-Galindo, C., George, D.J., Gilligan, T.D., et al. (2020). Clinical cancer advances 2020: annual report on progress against cancer from the American Society of Clinical Oncology. *J. Clin. Oncol.* *38*, 1081. <https://doi.org/10.1200/JCO.19.03141>.
- Kennedy, L.B., and Salama, A.K.S. (2020). A review of cancer immunotherapy toxicity. *CA Cancer J. Clin.* *70*, 86–104. <https://doi.org/10.3322/caac.21596>.
- Herrmann, J. (2020). Vascular toxic effects of cancer therapies. *Nat. Rev. Cardiol.* *17*, 503–522. <https://doi.org/10.1038/s41569-020-0347-2>.
- Lin, L., Sabnis, A.J., Chan, E., Olivias, V., Cade, L., Pazarentzos, E., Asthana, S., Neel, D., Yan, J.J., Lu, X., et al. (2015). The Hippo effector YAP promotes resistance to RAF- and MEK-targeted cancer therapies. *Nat. Genet.* *47*, 250–256. <https://doi.org/10.1038/ng.3218>.
- Lewis, J.E., Forshaw, T.E., Boothman, D.A., Furdai, C.M., and Kemp, M.L. (2021). Personalized genome-scale metabolic models identify targets of redox metabolism in radiation-resistant tumors. *Cell Syst.* *12*, 68–81.e11. <https://doi.org/10.1016/j.cels.2020.12.001>.
- Yeldag, G., Rice, A., and del Rio Hernandez, A. (2018). Chemoresistance and the self-maintaining tumor microenvironment. *Cancers* *10*, 471. <https://doi.org/10.3390/cancers10120471>.
- Steg, A.D., Bevis, K.S., Katre, A.A., Ziebarth, A., Dobbin, Z.C., Alvarez, R.D., Zhang, K., Conner, M., and Landen, C.N. (2012). Stem cell pathways contribute to clinical chemoresistance in ovarian cancer. *Clin. Cancer Res.* *18*, 869–881. <https://doi.org/10.1158/1078-0432.CCR-11-2188>.
- McCarthy, E.F. (2006). The toxins of William B. Coley and the treatment of bone and soft-tissue sarcomas. *Iowa Orthop. J.* *26*, 154–158.
- Kramer, M.G., Masner, M., Ferreira, F.A., and Hoffman, R.M. (2018). Bacterial therapy of cancer: promises, limitations, and insights for future directions. *Front. Microbiol.* *9*, 16. <https://doi.org/10.3389/fmicb.2018.00016>.
- Datsenko, K.A., and Wanner, B.L. (2000). One-step inactivation of chromosomal genes in *Escherichia coli* K-12 using PCR products. *Proc. Natl. Acad. Sci. U S A* *97*, 6640–6645. <https://doi.org/10.1073/pnas.120163297>.
- Arrach, N., Cheng, P., Zhao, M., Santiviago, C.A., Hoffman, R.M., and McClelland, M. (2010). High-throughput screening for *Salmonella* avirulent mutants that retain targeting of solid tumors. *Cancer Res.* *70*, 2165–2170. <https://doi.org/10.1158/0008-5472.can-09-4005>.
- Mi, Z., Feng, Z.-C., Li, C., Yang, X., Ma, M.-T., and Rong, P.-F. (2019). *Salmonella*-mediated cancer therapy: an innovative therapeutic strategy. *J. Cancer* *10*, 4765–4776. <https://doi.org/10.7150/jca.32650>.
- Clairmont, C., Lee, K.C., Pike, J., Ittensohn, M., Low, K.B., Pawelek, J., Bermudes, D., Brecher, S.M., Margitich, D., Turnier, J., et al. (2000). Biodistribution and genetic stability of the novel antitumor agent VNP20009, a genetically modified strain of *Salmonella typhimurium*. *J. Infect. Dis.* *181*, 1996–2002. <https://doi.org/10.1086/315497>.
- Toso, J.F., Gill, V.J., Hwu, P., Marincola, F.M., Restifo, N.P., Schwartzentruber, D.J., Sherry, R.M., Topalian, S.L., Yang, J.C., Stock, F., et al. (2002). Phase I study of the intravenous administration of attenuated *Salmonella typhimurium* to patients with metastatic melanoma. *J. Clin. Oncol.* *20*, 142–152. <https://doi.org/10.1200/jco.2002.20.1.142>.
- Coutermarsh-Ott, S.L., Broadway, K.M., Scharf, B.E., and Allen, I.C. (2017). Effect of *Salmonella enterica* serovar Typhimurium VNP20009 and VNP20009 with restored chemotaxis on 4T1 mouse mammary carcinoma progression. *Oncotarget* *8*, 33601–33613. <https://doi.org/10.18632/oncotarget.16830>.
- Broadway, K.M., Modise, T., Jensen, R.V., and Scharf, B.E. (2014). Complete genome sequence of *Salmonella enterica* serovar Typhimurium VNP20009, a strain engineered for tumor targeting. *J. Biotechnol.* *192*, 177–178. <https://doi.org/10.1016/j.jbiotec.2014.07.006>.
- Zhao, M., Yang, M., Li, X.-M., Jiang, P., Baranov, E., Li, S., Xu, M., Penman, S., and Hoffman, R.M. (2005). Tumor-targeting bacterial therapy with amino acid auxotrophs of GFP-expressing *Salmonella typhimurium*. *Proc. Natl. Acad. Sci. U S A* *102*, 755–760. <https://doi.org/10.1073/pnas.0408422102>.
- Hoffman, R.M. (2016). Tumor-targeting *Salmonella typhimurium* A1-R: an overview. *Methods Mol. Biol.* *1409*, 1–8. https://doi.org/10.1007/978-1-4939-3515-4_1.
- Nemunaitis, J., Cunningham, C., Senzer, N., Kuhn, J., Cramm, J., Litz, C., Cavagnolo, R., Cahill, A., Clairmont, C., and Sznol, M. (2003). Pilot trial of genetically modified, attenuated *Salmonella* expressing the *E. coli* cytosine deaminase gene in refractory cancer patients. *Cancer Gene Ther.* *10*, 737–744. <https://doi.org/10.1038/sj.cgt.7700634>.
- Cunningham, C., and Nemunaitis, J. (2001). A phase I trial of genetically modified *Salmonella typhimurium* expressing cytosine deaminase (TAPET-CD, VNP20029) administered by intratumoral injection in combination with 5-fluorocytosine for patients with advanced or metastatic cancer. Protocol no: CL-017. Version: April 9, 2001. *Hum. Gene Ther.* *12*, 1594–1596.
- Gniadek, T.J., Augustin, L., Schottel, J., Leonard, A., Saltzman, D., Greeno, E., and Batist, G. (2020). A phase I, dose escalation, single dose trial of oral attenuated *Salmonella typhimurium* containing human IL-2 in patients with metastatic gastrointestinal cancers. *J. Immunother.* *43*, 217–221. <https://doi.org/10.1097/cji.0000000000000325>.
- Pulaski, B.A., and Ostrand Rosenberg, S. (2001). Mouse 4T1 breast tumor model. *Curr. Protoc. Immunol. Chapter 20*, Unit 20.2. <https://doi.org/10.1002/0471142735.im2002s39>.
- Gao, Z.-G., Tian, L., Hu, J., Park, I.-S., and Bae, Y.H. (2011). Prevention of metastasis in a 4T1 murine breast cancer model by doxorubicin carried by folate conjugated pH sensitive polymeric micelles. *J. Control Release* *152*, 84–89. <https://doi.org/10.1016/j.jconrel.2011.01.021>.
- Parveen, S., Siddharth, S., Cheung, L.S., Kumar, A., Shen, J., Murphy, J.R., Sharma, D., and Bishai, W.R. (2021). Therapeutic targeting with DABIL 4 depletes myeloid suppressor cells in 4T1 triple negative breast cancer model. *Mol. Oncol.* *15*, 1330–1344. <https://doi.org/10.1002/1878-0261.12938>.
- Aslakson, C.J., and Miller, F.R. (1992). Selective events in the metastatic process defined by analysis of the sequential dissemination of subpopulations of a mouse mammary tumor. *Cancer Res.* *52*, 1399–1405.

26. Cummings, M.C., Simpson, P.T., Reid, L.E., Jayanthan, J., Skerman, J., Song, S., McCart Reed, A.E., Kutasovic, J.R., Morey, A.L., Marquart, L., et al. (2014). Metastatic progression of breast cancer: insights from 50 years of autopsies. *J. Pathol.* 232, 23–31. <https://doi.org/10.1002/path.4288>.
27. Lorusso, G., and Ruegg, C. (2008). The tumor microenvironment and its contribution to tumor evolution toward metastasis. *Histochem. Cell Biol.* 130, 1091–1103. <https://doi.org/10.1007/s00418-008-0530-8>.
28. Felgner, S., Kocijancic, D., Frahm, M., and Weiss, S. (2016). Bacteria in cancer therapy: renaissance of an old concept. *Int. J. Microbiol.* 2016, 8451728. <https://doi.org/10.1155/2016/8451728>.
29. Tjuvajev, J., Blasberg, R., Luo, X., Zheng, L.M., King, I., and Bermudes, D. (2001). Salmonella-based tumor-targeted cancer therapy: tumor amplified protein expression therapy (TAPET™) for diagnostic imaging. *J. Control Release.* 74, 313–315. [https://doi.org/10.1016/s0168-3659\(01\)00340-6](https://doi.org/10.1016/s0168-3659(01)00340-6).
30. Kordes, A., Grahl, N., Koska, M., Preusse, M., Arce-Rodriguez, A., Abraham, W.-R., Kaefer, V., and Haussler, S. (2019). Establishment of an induced memory response in *Pseudomonas aeruginosa* during infection of a eukaryotic host. *ISME J.* 13, 2018–2030. <https://doi.org/10.1038/s41396-019-0412-1>.
31. Lambert, G., and Kussell, E. (2014). Memory and fitness optimization of bacteria under fluctuating environments. *PLoS Genet.* 10, e1004556. <https://doi.org/10.1371/journal.pgen.1004556>.
32. Gokhale, C.S., Giaimo, S., and Remigi, P. (2021). Memory shapes microbial populations. *PLoS Comput. Biol.* 17, e1009431. <https://doi.org/10.1371/journal.pcbi.1009431>.
33. Badawy, A.A.B. (2018). Targeting tryptophan availability to tumors: the answer to immune escape? *Immunol. Cell Biol.* 96, 1026–1034. <https://doi.org/10.1111/imcb.12168>.
34. Pavlova, N.N., and Thompson, C.B. (2016). The emerging hallmarks of cancer metabolism. *Cell Metab.* 23, 27–47. <https://doi.org/10.1016/j.cmet.2015.12.006>.
35. Zhao, M., Geller, J., Ma, H., Yang, M., Penman, S., and Hoffman, R.M. (2007). Monotherapy with a tumor-targeting mutant of *Salmonella typhimurium* cures orthotopic metastatic mouse models of human prostate cancer. *Proc. Natl. Acad. Sci. U S A* 104, 10170–10174. <https://doi.org/10.1073/pnas.0703867104>.
36. Sung, H., Ferlay, J., Siegel, R.L., Laversanne, M., Soerjomataram, I., Jemal, A., and Bray, F. (2021). Global cancer statistics 2020: GLOBOCAN estimates of incidence and mortality worldwide for 36 cancers in 185 countries. *CA. Cancer J. Clin.* 71, 209–249. <https://doi.org/10.3322/caac.21660>.
37. Nagakura, C., Hayashi, K., Zhao, M., Yamauchi, K., Yamamoto, N., Tsuchiya, H., Tomita, K., Bouvet, M., and Hoffman, R.M. (2009). Efficacy of a genetically-modified *Salmonella typhimurium* in an orthotopic human pancreatic cancer in nude mice. *Anticancer Res.* 29, 1873–1878.
38. Biswas, S.K., Allavena, P., and Mantovani, A. (2013). Tumor-associated macrophages: functional diversity, clinical significance, and open questions. *Semin. Immunopathol.* 35, 585–600.
39. Kelly, P.M.A., Davison, R.S., Bliss, E., and McGee, J. (1988). Macrophages in human breast disease: a quantitative immunohistochemical study. *Br. J. Cancer* 57, 174–177. <https://doi.org/10.1038/bjc.1988.36>.
40. Lewis, C.E., Leek, R., Harris, A., and McGee, J. (1995). Cytokine regulation of angiogenesis in breast cancer: the role of tumor associated macrophages. *J. Leukoc. Biol.* 57, 747–751. <https://doi.org/10.1002/jlb.57.5.747>.
41. Zhang, W.-j., Wang, X.h., Gao, S.t., Chen, C., Xu, X.y., sun, Q., Zhou, Z.h., Wu, G.z., Xu, G., Yao, Y.-Z., and Guan, W.X. (2018). Tumor-associated macrophages correlate with phenomenon of epithelial-mesenchymal transition and contribute to poor prognosis in triple-negative breast cancer patients. *J. Surg. Res.* 222, 93–101. <https://doi.org/10.1016/j.jss.2017.09.035>.
42. He, K.-F., Zhang, L., Huang, C.-F., Ma, S.-R., Wang, Y.-F., Wang, W.-M., Zhao, Z.-L., Liu, B., Zhao, Y.-F., Zhang, W.-F., and Sun, Z.J. (2014). CD163+ tumor-associated macrophages correlated with poor prognosis and cancer stem cells in oral squamous cell carcinoma. *Biomed. Res. Int.* 2014, 838632. <https://doi.org/10.1155/2014/838632>.
43. Sugimura, K., Miyata, H., Tanaka, K., Takahashi, T., Kurokawa, Y., Yamasaki, M., Nakajima, K., Takiguchi, S., Mori, M., and Doki, Y. (2015). High infiltration of tumor associated macrophages is associated with a poor response to chemotherapy and poor prognosis of patients undergoing neoadjuvant chemotherapy for esophageal cancer. *J. Surg. Oncol.* 111, 752–759. <https://doi.org/10.1002/jso.23881>.
44. Zhang, J., Yan, Y., Yang, Y., Wang, L., Li, M., Wang, J., et al. (2016). High infiltration of tumor-associated macrophages influences poor prognosis in human gastric cancer patients, associates with the phenomenon of EMT. *Medicine* 95, e2636.
45. Kirthika, P., Senevirathne, A., Jawalagatti, V., Park, S., and Lee, J.H. (2020). Deletion of the lon gene augments expression of *Salmonella* Pathogenicity Island (SPI)-1 and metal ion uptake genes leading to the accumulation of bactericidal hydroxyl radicals and host pro-inflammatory cytokine-mediated rapid intracellular clearance. *Gut Microbes* 11, 1695–1712. <https://doi.org/10.1080/19490976.2020.1777923>.
46. Giulietti, A., Overbergh, L., Valckx, D., Decallonne, B., Bouillon, R., and Mathieu, C. (2001). An overview of real-time quantitative PCR: applications to quantify cytokine gene expression. *Methods* 25, 386–401. <https://doi.org/10.1006/meth.2001.1261>.
47. Harbor, C.S. (2010). M9 minimal medium (standard). Cold Spring Harb. Protoc. http://cshprotocols.cshlp.org/content/2010/8/pdb.rec12296.full?text_only=true.
48. Livak, K.J., and Schmittgen, T.D. (2001). Analysis of relative gene expression data using real-time quantitative PCR and the 2⁻ΔΔCT method. *Methods* 25, 402–408. <https://doi.org/10.1006/meth.2001.1262>.
49. Jawalagatti, V., Kirthika, P., Hewawaduge, C., Park, J.-Y., Yang, M.S., Oh, B., So, M.Y., Kim, B., and Lee, J.H. (2022). A simplified SARS-CoV-2 mouse model demonstrates protection by an oral replicon-based mRNA vaccine. *Front. Immunol.* 13, 465. <https://doi.org/10.3389/fimmu.2022.811802>.